

Multibeam Sonar-Based Navigation of Small UUVs for MCM Purposes

Nikola Mišković* Vladimir Djapic** Đula Nađ* Zoran Vukić*

** University of Zagreb, Faculty of Electrical Engineering and Computing, LabUST - Laboratory for Underwater Systems and Technologies*

Unska 3, Zagreb, Croatia

(e-mail: nikola.miskovic@fer.hr)

*** NATO Undersea Research Centre (NURC)*

Viale S. Bartolomeo 400, La Spezia 19126, Italy

(e-mail: djapic@nurc.nato.int)

Abstract Autonomous vehicles (AxV), surface (ASV) and underwater (AUV), are being considered for the following maritime security missions: Mine Countermeasures (MCM) and Harbor Protection (HP). Applicable threats include attack swimmers/divers, bottom and moored mines, mines or improvised explosive devices placed on pilings, quays, or hulls of ships at anchor or in port. This article focuses on solutions for mine reacquisition and neutralization (RN). One concept for an overall RN system is two collaborating vehicles, an AxV and a unmanned underwater vehicle (UUV). The main task of the RN AxV is to reacquire a bottom target with multibeam imaging sonar, maintain distance while pointing at the target, and perform circular inspection around a target while varying the circle diameter. The main task of the RN UUV is to converge towards the desired line once deployed from the AxV. UUV guiding is accomplished by automatically processing sonar imagery onboard of the AxV and passing sonar position, and UUV range and bearing information to the UUV which processes this information to drive itself to the desired location.

Keywords: Marine system navigation, guidance and control; Autonomous underwater vehicles; Unmanned marine vehicles

1. INTRODUCTION

The state of the art in operational maritime autonomous unmanned platforms is currently limited to executing missions pre-planned by an operator. Thereafter, human operators must intervene to observe events, make decisions and guide the vehicle in achieving its mission. An example of a pre-programmed mission performed by AUVs is the detection and classification phase of an MCM mission. The current generation of AUVs is capable of following an arbitrary polygon or lawn-mower pattern, recording data of sidescan or synthetic aperture sonar (SAS) sensors. This article assumes that a survey has been done by an AUV equipped with SAS sensor. Super classification is defined as the ability to recognize mines at long range with sufficient confidence to proceed to mine reacquisition & neutralization. Typical classification image of wedge and cylindrical targets based on 3D reconstruction techniques and multiple target look using wideband SAS are shown in article, Groen et al. (2010). NURC has an AUV with

mine detection and classification capability which is used for Search-Classify-Map (SCM) mission of the MCM. Currently, the selection of which contact to investigate, reacquire, and neutralize is done by an operator through a post-mission analysis of SAS data. In the future, when Automatic Target Recognition (ATR) algorithms become mature, the "address" (i.e. positional info of the interesting target) can be passed via acoustic link to the reacquisition & neutralization platform.

The navigation capability for most modern AUVs is provided by an aided inertial navigation system (AINS). An AINS is based around an inertial navigation system (INS) aided by a doppler velocity log (DVL), depth sensor and global positioning system (GPS). The aiding sensors are included to either reduce the drift rate (the DVL is used to bound the velocity estimate whilst the pressure sensor bounds the vertical channel) or to periodically re-set position estimates (GPS). The modern INS systems were specified as being capable of heading drift rates of less than 0.01deg/hr accuracy, Baralli et al. (2007). The high accuracy comes with higher cost, which is acceptable for mine search missions since the AUV is not expendable, but not desired for mine neutralization for which the expendable (one-shot) vehicles are considered. Furthermore, higher frequency LBL systems can offer sub-centimeter precision and update rates up to 10 Hz, Kinsey et al. (2006). GPS Intelligent Buoys (GIB) systems offer adequate perfor-

* The work was carried out in the framework of a Coordination and Support Action type of project supported by European Commission under the Seventh Framework Programme "CURE - Developing Croatian Underwater Robotics Research Potential" SP-4 Capacities (call FP7-REGPOT-2008-1) under Grant Agreement Number: 229553.

**This work was also supported by North Atlantic Treaty Organisation via NURC's SPOW - Scientific Programme of Work.

mance without need for precisely mooring transponders on the sea-floor, Alcocer et al. (2004). However, transponder deployment and recovery is still necessary, and this task could prove problematic for the autonomous vehicle. This can be avoided by using a USBL system. However, in shallow water, performance of these systems degrades with higher elevation angle.

The concept of using multibeam imaging sonar for UUV navigation aiding offers satisfactory results at much lower cost. It can detect range and bearing of the UUV relative to the head, similarly to a USBL system. However, higher resolution offers better precision in comparison to the USBL system. The downside is that the UUV has to be in the sonar field-of-view in order to be detected. This can be solved by using a pan and tilt platform with the sonar in order to ensure the UUV remains visible. In this case, the UUV that carries a mine neutralization payload can be a small and inexpensive underwater unit with the least sensors possible (depth sensor, compass and an acoustic receiver).

Other research has been done using multibeam imaging sonar for AUV navigation, Folkesson et al. (2008). The functionality includes feature tracking and global localization using a simultaneous localization and mapping (SLAM) algorithm. Our approach differs from those since in our case multibeam sonar resides on external platform and it is not a part of the necessary sensor suite on the AUV.

1.1 Collaborative Autonomous Vehicles

The goal of this article is to introduce the potential of using collaborative autonomous vehicles in MCM scenarios. The collaborative use of autonomous systems has the potential to transform MCM capability, from legacy systems focused on clearance with surface ships (50 sailors working in a minefield) to quickly deployable systems. It is designed to be scalable to the needs of the operation and to offer an order of magnitude increase in the tempo of operations and reduction in through-life costs keeping men out of the mine field.

In the envisioned concept of operations, an autonomous vehicle reacquires a previously identified target (in the hunting phase) using its imaging sonar. The vehicle then initiates an adaptive engagement plan autonomously, or it may be controlled by an operator. The vehicle tracks, scans and maintains the target in the field of view of the imaging sonar, while compensating for wind, waves and currents. Next, the vehicle guides a low-cost neutralization UUV to carry a payload to neutralize the target. This concept is shown in Fig. 1 (left). We have a collaboration of a completely autonomous vehicle (ASV in our case) which has a reliable, accurate, and robust navigation sensor suite that enable it to sense the environment and an expendable underwater vehicle (UUV) which lacks the sophisticated sensors but can automatically drive itself if sensor aiding comes from a more capable platform. The typical sonar imagery with the UUV in the field-of-view of sonar is shown in Fig. 1 (right). UUV guiding is accomplished by automatically processing sonar imagery onboard the ASV and passing sonar position, UUV range and bearing

information to the UUV which processes this information to drive itself to the desired location.

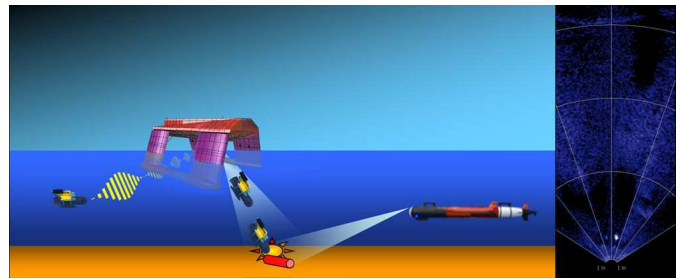


Figure 1. Mine reacquisition and neutralization: a highly capable SWATH ASV or hover-capable AUV guiding a low-cost expendable UUV to the sea mine (left); automated UUV (white dot) tracking from the sonar imagery (right).

1.2 System description

The automatic UUV The automatic UUV is a modification of the VideoRay Pro IV submersible, as shown in Fig. 2. An additional pressure vessel attached to the bottom of the ROV is equipped with a PC board, batteries, additional electronic components and an acoustic receiver. In the current version, a thin cable is used to communicate with the ground station instead of the acoustic link. A small cartridge at the top of the ROV contains a GPS module used for surface navigation.

The main task of the UUV is to converge towards the desired line once deployed. The sensor suite on the UUV is inadequate to correctly calculate horizontal and vertical distance from the desired line. Therefore, in order to ensure line following, position information is provided from the ASV equipped with a forward looking multibeam sonar.

The forward looking multibeam sonar The target area for the proposed application is about $100m \times 100m$. Processing the sonar image is difficult in a cluttered environment. Adding a passive reflector to the UUV can ease this task. The assumption is made that the UUV starts the mission in the vicinity of the sonar head to reduce the number of false reflections during initial detection. This improves performance and aids in dismissing false readings. Currently, sonar image processing is based on adaptive thresholding and area filtering. The search window was selected empirically based on the image resolution and vehicle speed. This proved to be adequate for testing in real-life conditions where the vehicle moves with slow constant speed.



Figure 2. The UUV developed for the MCM mission.

The concept of using a multibeam sonar for navigation aiding has given good results. Robustness and accuracy of position estimation is dependent directly on image processing. Errors like misalignments and image calibration can be removed with careful setup. More time will be invested in increasing robustness. Estimation of the next UUV position in the sonar image will improve detection when more than one candidate is detected. This also incorporates the UUV movement into processing which means that strong static reflections can be easily filtered out. Dynamic selection of search window size dependent on the estimation quality and image resolution will also improve performance and robustness when different frequency sonars are tested.

2. MISSION SCENARIO

The main motivation for this type of mission scenario and system configuration is to have 1) a small, inexpensive, and expendable UUV with least sensors possible (depth sensor, compass and an acoustic receiver) and 2) a remote observing and sensing surface platform which guides the underwater vehicle to the target using sonar imagery (ASV).

Once the ASV spots the target within the onboard multi-beam sonar image, two coordinates in the Earth frame are recorded: coordinates of the ASV $T_1 = (x_1, y_1, z_1) = (x_c, y_c, z_c)$ and coordinates of the target $T_2 = (x_2, y_2, z_2)$ (the assumption is that the depth of the target is known). These two points allow setting a desired line from T_1 to T_2 as it is shown in Fig. 3(a). This 3D line stays intact during the whole mission, regardless of the possible drift of the ASV. At this point, the UUV is launched from the ASV and separate algorithms are performed, as shown in Fig. 4.

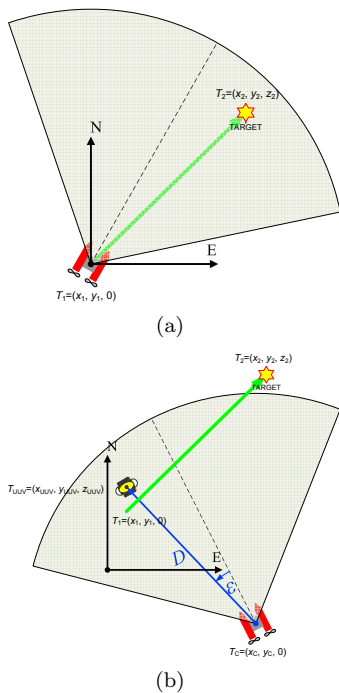


Figure 3. Mission scenario (a) before and (b) after the UUV is deployed.

Onboard the ASV, range D and bearing ε of the UUV with respect to the sonar head are determined from the sonar image (see Fig. 3(b)). Then the ASV sends the coordinates of the vehicle x_c and y_c , range D and $\psi_c + \varepsilon$ where ψ_c is the heading of the ASV at a rate of 0.5 Hz, depending on the quality of the acoustic modem link. The number of data which are sent to the UUV has to be minimized due to the limited bandwidth of such modems.

Onboard the UUV, simultaneously, the following algorithm is executed, with an update rate of 10Hz. If a packet from the ASV is available, D , x_c , y_c and $\psi_c + \varepsilon$ are received. Locating the UUV in the sonar image does not provide enough information for 3D localization. By adding the depth z_{UUV} (available at the UUV), equations (1) and (2) are used to calculate the real position. Based on this position horizontal and vertical distances to the desired line are estimated.

$$x_{UUV} = x_c + \cos(\psi_c + \varepsilon) \sqrt{D^2 - z_{UUV}^2} \quad (1)$$

$$y_{UUV} = y_c + \sin(\psi_c + \varepsilon) \sqrt{D^2 - z_{UUV}^2} \quad (2)$$

When deploying the UUV, the EKF is initialized. Knowing the deployment location and the desired target, line parameters are calculated and the line following model is initialized. System identification using self-oscillations, Mišković et al. (2009), is performed on the UUV, and the dynamic parameters (which are used in the EKF and the controllers) of the vehicle model are determined. The EKF estimates onboard the UUV are corrected using the measurements. The measurements might not be available for two reasons: either the acoustic link failed, or due to the faster sampling rate onboard the UUV. In any case, EKF outputs are used to estimate distances to the line.

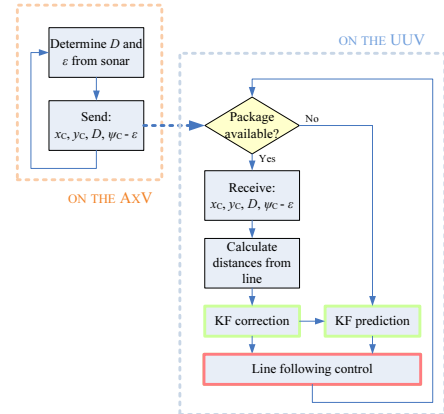


Figure 4. Schematic description of the algorithms performed onboard the ASV and the UUV during the mission.

Remarks. The main advantages of the proposed system configuration are as follows:

- (1) This approach utilizes one way communication between the UUV and the ASV. Any other approach would require UUV sending its depth to the ASV.
- (2) The proposed Kalman filtering enables UUV navigation in the cases when measurements are not available.

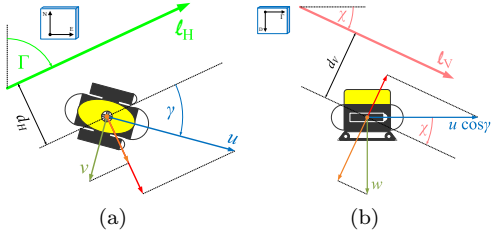


Figure 5. Line following model in (a) the $z = z_0$ and (b) the vertical plane.

- (3) The multibeam sonar mounted on the ASV need not have the target and the UUV in the field of view at all times, but only the UUV. If the target is in the field of view, corrected target position can optionally be sent to the UUV.
- (4) If the ASV drifts due to winds, waves, or currents, the linear path remains stationary hence the UUV movement will not be affected by the drift.

3. MATHEMATICAL MODELING

3.1 3D line following problem formulation

Let the North-East-Down (NED) coordinate frame be positioned in such a way that its origin is always at the same depth as the depth of the UUV. Let the oriented 3D line ℓ , which is supposed to be followed, be defined by two points T_1 and T_2 and let the position of the UUV be defined with a point T_{UUV} . Then, the 3D line following problem can be observed as following two lines simultaneously:

- the oriented horizontal line ℓ_H defined with T_1 and angle Γ in the N-D plane, and
- the oriented vertical line ℓ_V defined with T_1 and angle χ in the N-E plane.

3.2 Line following mathematical model

The line following problem formulation is derived for the specific case of the thruster allocation as in the case of the observed UUV, and the details can be found in Mišković et al. (2010).

The ℓ_H line following model The scheme for following the line ℓ_H is shown in Fig. 5(a) and the equations follow.

$$\dot{d}_H = u \sin \gamma + v \cos \gamma + \xi_H \quad (3)$$

$$\dot{\gamma} = r \quad (4)$$

$$\dot{r} = -\frac{\beta(r)}{\alpha_r} r + \frac{k_{ru}}{\alpha_r} r u + \frac{1}{\alpha_r} N \quad (5)$$

The attack angle $\gamma = \psi - \Gamma$ is controlled in such a way that the vehicle approaches the line, causing the distance d_H to converge to 0. Surge speed u is not measured but it is assumed to be constant given a constant surge force X_{ref} . Sway speed v cannot be controlled in the given vehicle configuration, therefore the term $v \cos \gamma$ can be considered as an external disturbance (together with ξ_H) which has to be compensated for. The yaw dynamics are given in (5) where α_r is yaw inertia and $\beta(r)$ is yaw drag, which is

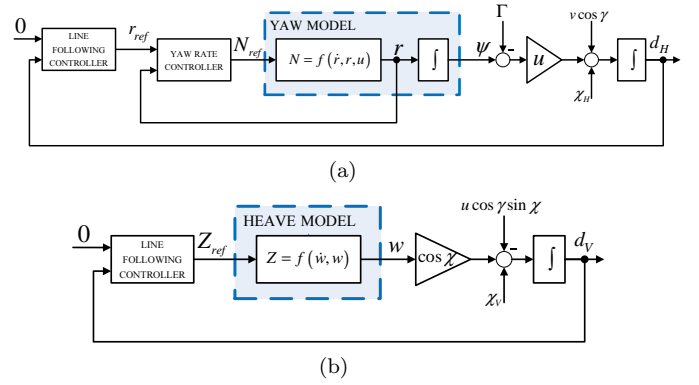


Figure 6. The ℓ_H and ℓ_V line following control structures.

assumed to be purely constant or linear. During the real experiments with the UUV it was shown that the coupling between r and surge speed u cannot be neglected but has to be compensated for within the control algorithm. The conclusion is made that this is the case due to the hydrodynamic characteristics of the UUV.

The ℓ_V line following model The scheme for following the line ℓ_V is shown in Fig. 5(b) and the equations follow (the figure shows the situation when the UUV is aligned with ℓ_H , i.e. $\Gamma = \psi$).

$$\dot{d}_V = w \cos \chi - u \cos \gamma \sin \chi + \xi_V \quad (6)$$

$$\dot{w} = -\frac{\beta(w)}{\alpha_w} w + \frac{1}{\alpha_w} (Z + W - B) \quad (7)$$

The distance with regard to ℓ_V changes due to surge u and heave speed w , and the equation is given with (6). Parameter ξ_V presents any external disturbance and unmodelled dynamics in the system. Heave dynamics are given in (7) with B being buoyancy and W weight of the UUV.

4. CONTROL DESIGN

4.1 The ℓ_H line following controller

The line following controllers which are used in this work were introduced in Caccia et al. (2000). The controller consists of an inner yaw rate controller and outer line following controller, as it is shown in Fig. 6(a) where a linearized system in the kinematic model is assumed, i.e. $\sin \gamma \approx \gamma$. This approach assumes that direct actuator control is possible (given the observed vehicle) even though this is not always the case, Mišković et al. (2009).

The proposed controller ensures zero steady state error and compensation of external disturbances. The inner loop yaw rate controller is augmented with a term which compensates for the coupling effects in the yaw dynamic model (5), i.e. the $k_{ru} r u$ term. Since surge speed u is not measured, the assumption is made that $u \sim X_{ref}$ where X_{ref} is the commanded surge thrust. Under the assumption that $r_{ref} \approx r$, the feedforward term $k_{ru} X_{ref} r_{ref}$ is introduced into the controller:

$$N_{ref} = K_{Ir} \int_0^t (r_{ref} - r) dt - [K_{Pr} - \beta(r)] r + \tilde{k}_{ru} r_{ref} X_{ref} \quad (8)$$

The line following controller is of PD (proportional-derivative) type given by

$$r_{ref} = K_{Ph}(d_{H,ref} - d_H) + K_{Dh} \frac{d}{dt}(d_{H,ref} - d_H), \quad (9)$$

under the assumption that $d_{H,ref}$ is 0, i.e., convergence to the line is required. The controller parameters are determined using a model-based approach, from the closed loop transfer function (10) where a_{4h} , a_{3h} , a_{2h} and a_{1h} are desired line following closed loop transfer function parameters.

$$\frac{d_h}{d_{h,ref}} = \frac{1 + \frac{K_{Dh}}{K_{Ph}}s}{\underbrace{\frac{\alpha_r}{uK_{Ir}K_{Ph}}}_{a_{4h}}s^4 + \underbrace{\frac{K_{Pr}}{uK_{Ir}K_{Ph}}}_{a_{3h}}s^3 + \underbrace{\frac{1}{uK_{Ph}}}_{a_{2h}}s^2 + \underbrace{\frac{K_{Dh}}{K_{Ph}}}_{a_{1h}}s + 1} \quad (10)$$

The controller parameters follow as:

$$K_{Ir} = \frac{a_{2h}}{a_{4h}}\alpha_r, K_{Pr} = \frac{a_{3h}}{a_{4h}}\alpha_r, K_{Ph} = \frac{1}{ua_{2h}}, K_{Dh} = \frac{a_{1h}}{ua_{2h}}. \quad (11)$$

4.2 The ℓ_V line following controller

The proposed control structure for ℓ_v line following controller is shown in Fig. 6(b).

The controller algorithm is of I-PD type given with (12) where the output is the desired heave force Z_{ref} . This algorithm is equal to the classical *PID* controller if $d_{V,ref} = 0$ is required.

$$Z_{ref} = K_{Iv} \int_0^t (d_{V,ref} - d_V) dt - K_{Pv}d_V - \frac{d}{dt}d_V \quad (12)$$

Similarly, as in the case of the ℓ_H line following controller, the model-based approach is used where (13) is the desired closed loop with a_{3v} , a_{2v} and a_{1v} being the tunable parameters.

$$\frac{d_v}{d_{v,ref}} = \frac{1}{\underbrace{\frac{\alpha_w}{K_{Iv} \cos \chi}}_{a_{3v}}s^3 + \underbrace{\frac{\beta_w + K_{Dv} \cos \chi}{K_{Iv} \cos \chi}}_{a_{2v}}s^2 + \underbrace{\frac{K_{Pv}}{K_{Iv}}}_{a_{1v}}s + 1} \quad (13)$$

From here follow the controller parameters:

$$K_{Iv} = \frac{\alpha_w}{\cos \chi} \frac{1}{a_{v3}}, K_{Pv} = \frac{\alpha_w}{\cos \chi} \frac{a_{v1}}{a_{v3}}, K_{Dv} = \frac{\alpha_w}{\cos \chi} \frac{a_{v2}}{a_{v3}} - \frac{\beta_w}{\cos \chi}. \quad (14)$$

The choice of the desired closed loop function parameters depend on the feasible dynamics of the underwater vehicle.

4.3 UUV navigation

UUV navigation uses the Extended Kalman Filter (EKF) for state estimation. The mathematical model described in Section 3 is used in the estimator. Outputs of the estimator are horizontal and vertical distances from the line. Additionally, compass and pressure sensor information is filtered as well.

After the EKF initialization, line following is engaged. Estimator outputs are used as feedback values for the controller. Estimations are output with 10 Hz. Measurements received from the ASV limit the drift of the estimator. Frequency of the received measurements is varying due to the communication channel but has a minimum value of 0.5 Hz.

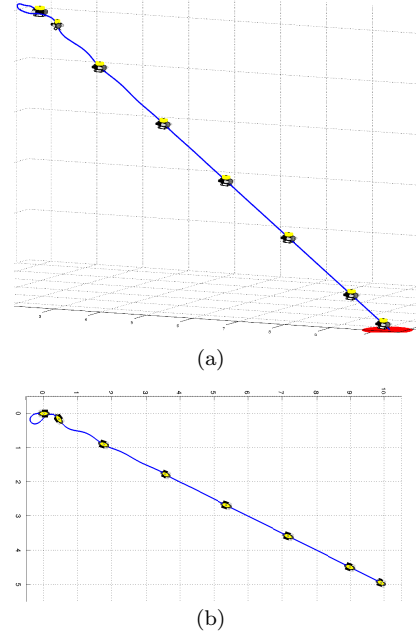


Figure 7. Simulation results of the UUV following a straight line to the target area (red circle) – (a) the 3D view and (b) the topside view.

5. RESULTS

5.1 Simulation results

The simulation results were obtained by using a coupled model of the UUV with an update measurement from the sonar every 1 s. The control is performed at a rate of 10 Hz. The simulation results presented in Fig. 7 are obtained while the ASV was moving with forward speed $u = 0.1\text{m/s}$ and lateral speed due to currents $v = 0.015\text{m/s}$. The target position is chosen at the coordinates $T_2 = (10, 5, -5)$ with $T_1 = (0, 0, 0)$. The simulation results show that the vehicle is behaving as expected even when the multibeam sonar carrier (the reference point) is mobile, as long as the UUV is in the field of view.

5.2 Field-test results

The experimental results, obtained on several occasions in La Spezia, Italy and Murter, Croatia are shown in Figs. 8 and 9. Fig. 9 shows the UUV traces in time in the sonar image. The full real time video is submitted with the paper and can be downloaded directly at lapost.fer.hr/media/movies/multibeam_sonar.mpeg. It is worth noting how the UUV converges to the desired line.

Fig. 8 shows the time responses of a different experiment where initial position of the UUV was 2 meters away from the desired line with the UUV almost aligned with the line. Fig. 8 shows the horizontal distance to the line and the heading of the vehicle – both are converging to the desired values.

The field experiments have shown that lower resolution (and lower cost) sonar feedback can be used for guiding a simplified mine neutralization UUV to the moored or bottom mine since the mine has already been detected and classified during the prior super classification mission.

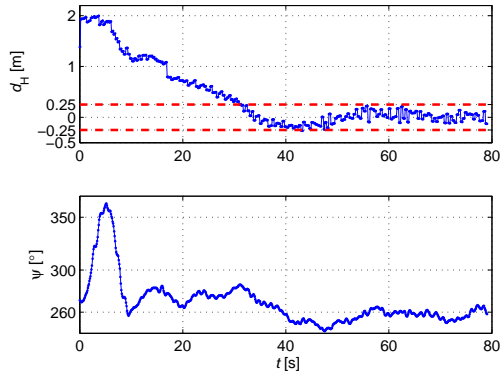


Figure 8. Performance of the UUV during experimental trials – horizontal distance d_H and UUVs heading ψ .

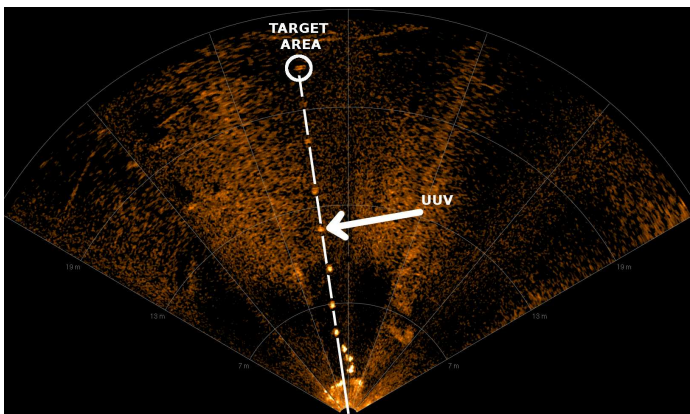


Figure 9. Multibeam sonar image with UUV traces in time as a result of field experiments.

Again, for the mine neutralization mission, as the automatic sonar image processing algorithms are being more mature they will be considered to make a decision on target detection instead of the operator during the target reacquisition phase.

6. CONCLUSION

This paper describes results which show potential for collaborative use of autonomous vehicle in MCM. A common goal has been the employment of autonomous vehicle executing autonomous behaviors to minimize the workload on the operator. Our prototype autonomous systems are designed to be scalable to the needs of the operation and to offer an increase in the tempo of operations and reduction of lifecycle costs.

We mentioned before that range and bearing information need to be transmitted regularly to the UUV. During initial testing a tethered connection was used, both for convenience and safety. This drastically eased data transmission. Tethered communication was reliable and had negligible transmission delay. Both of these are not present when switching to acoustic communication. The reliability issue is tackled by using robust transmission protocols. Performance of systems available for the project are around 20 bps of payload data. This means that transmission delays are around 2 seconds. Acoustic communication between

the ASV and UUV is currently being implemented and tested.

We anticipate that delayed measurement corrections and periodic dropouts will have a negative impact on the Kalman filter estimate. To alleviate this problem, in future work, we will extend the Kalman filter with backward and forward temporal propagation, meaning that while measurement corrections are not available, we propagate the filter purely on a priori estimates. In the meantime we are storing these propagations. Once a measurement arrives we go back to the time the measurement was taken and correct the a priori estimate. Then we propagate to the current time period and continue the process. Similar implementations have already been done before, Alcocer et al. (2004) and Miller et al. (2010). In addition, in future work, we will address the possibility of UUV exiting the field-of-view of a sonar due to external disturbances acting on the ASV (causing pitch and roll) by advancing the pan and tilt controllers and the design of moving target reacquisition behaviors for the ASV.

ACKNOWLEDGEMENTS

The success of the experiments reported in this article owes great credit to the computer programmers, engineering team, and technicians who integrated new functionality into the vehicles and kept them operational in sometimes difficult operating environments, especially Dr. Stefano Fioravanti, Arjan Vermeij and Alberto Grati from NURC.

REFERENCES

- Alcocer, A., Oliveira, P., and Pascoal, A. (2004). Study and implementation of an EKF GIB-based underwater positioning system. In *IFAC CAMS04*.
- Baralli, F., Evans, B., Coiras, E., and Bellettini, A. (2007). AUV navigation for MCM operations. Technical report, NATO Undersea Research Centre, La Spezia, Italy.
- Caccia, M., Indiveri, G., and Veruggio, G. (2000). Modelling and identification of open-frame variable configuration unmanned underwater vehicles. *IEEE Journal of Oceanic Engineering*, 25(2), 227–240.
- Folkesson, J., Leederkerken, J., Williams, R., Patrikalakis, A., and Leonard, J. (2008). *A Feature Based Navigation System for an Autonomous Underwater Robot*. Tracts in Advanced Robotics. Springer, Berlin.
- Groen, J., Coiras, E., and Williams, D. (2010). False-alarm reduction in mine classification using multiple looks from a synthetic aperture sonar. In *IEEE OCEANS*.
- Kinsey, J.C., Eustice, R.M., and Whitcomb, L.L. (2006). A survey of underwater vehicle navigation: recent advances and new challenges. In *proceedings of 7th IFAC Conference on Manoeuvring and Control of Marine Craft*.
- Miller, P., Farrell, J., Zhao, Y., and Djapic, V. (2010). Autonomous underwater vehicle navigation. *IEEE Journal of Ocean Engineering*, 35(3), 663 – 678.
- Mišković, N., Bibuli, M., Bruzzone, G., Caccia, M., and Vukić, Z. (2009). Tuning marine vehicles' guidance controllers through self-oscillation experiments. *Proceedings of the MCMC'09 Conference*.
- Mišković, N., Nađ, Đ., and Vukić, Z. (2010). 3D line following for unmanned underwater vehicles. *Brodogradnja : časopis brodogradnje i brodograđevne industrije*, 61(2), 121–129.